Complex of heavy magnetic ions and luminescent silicon nanoparticles

Hoang, T.; Stupca, M.; Mantey, K.; Maximenko, Y.; Elhalawany, N.; Carr, C. M.; Yu, H.; Nayfeh, M. H.; Morgan, H.

Published in:
Journal of Applied Physics

DOI:
10.1063/1.4826635

Publication date:
2013

Citation for published version (APA):
Hoang, T., Stupca, M., Mantey, K., Maximenko, Y., Elhalawany, N., Carr, C. M., Yu, H., Nayfeh, M. H., & Morgan, H. (2013). Complex of heavy magnetic ions and luminescent silicon nanoparticles. *Journal of Applied Physics*, *114*(16), [164319]. https://doi.org/10.1063/1.4826635

Complex of heavy magnetic ions and luminescent silicon nanoparticles

T. Hoang, M. Stupca, K. Mantey, Y. Maximenko, N. Elhalawany, C. Carr, H. Yu, M. H. Nayfeh, and H. Morgan

Citation: Journal of Applied Physics **114**, 164319 (2013); doi: 10.1063/1.4826635
View online: http://dx.doi.org/10.1063/1.4826635
View Table of Contents: http://scitation.aip.org/content/aip/journal/jap/114/16?ver=pdfcov
Published by the AIP Publishing

Complex of heavy magnetic ions and luminescent silicon nanoparticles

T. Hoang,[1] M. Stupca,[1] K. Mantey,[1] Y. Maximenko,[1] N. Elhalawany,[2] C. Carr,[1] H. Yu,[1] M. H. Nayfeh,[1] and H. Morgan[3]
[1]*Department of Physics, University of Illinois at Urbana-Champaign, Urbana, Illinois 61801, USA*
[2]*Polymers and Pigments Department, Chemical Industrial Division, National Research Center, Cairo 12311, Egypt*
[3]*Department of Mathematics and Physics, Aberystwyth University, Aberystwyth, Ceredigion, SY23 3BZ, United Kingdom*

(Received 18 July 2013; accepted 8 October 2013; published online 30 October 2013)

We study the optical properties of luminescent silicon nanoparticles in the presence of magnetic ions of iron or erbium under wet conditions and electric biasing. Upon the introduction of the ions under zero biasing, the brightness is enhanced with some spectral change. Under biasing including breakdown field conditions, the enhancement remains stable and is maintained after recovery of the particles into nanosolid films using electric spray. The ion-nanoparticle interaction is analyzed using first principle atomistic calculations employing unrestricted Hartree-Fock density functional theory. The calculations yield configurations, which show strong binding and stability. The complexes promise diverse applications in magnetic/optical imaging, spatially programmable deposition, spin-based memories and transistors, infrared communications, filtration, as well as interplanetary and interstellar observation and modeling. © *2013 AIP Publishing LLC*.
[http://dx.doi.org/10.1063/1.4826635]

I. INTRODUCTION

The discovery of unique electronic and optical properties of nanometer scale crystalline silicon nanoparticles has opened new possibilities for silicon in technological applications and basic science.[1–3] Unlike bulk silicon which is an indirect gap dull semiconductor, silicon nanoparticles exhibit strong optical interaction including size dependent fluorescence. Additionally, bound complex formation of nanoparticles with ions provide some change in energy levels that can afford interesting non-optical applications such as memory devices[4] or electrochemical sensors.[5–7] For instance, interactions of silicon nanoparticles with ions, i.e., complex formation, can be exploited for detection of biological molecules such as glucose,[5–7] or electric current generation such as biofuel cells via charge transfer mechanisms,[8,9] or patterned deposition,[10] or addressing unexplained spectral phenomena in the galaxies pertaining to interplanetary and interstellar media.[11–16] The interaction of immobilized Si nanoparticles with Er ions embedded in a silicon oxide substrate in a non-complex configuration with nanoparticle-ion interspacing of several angstroms (10 Å for example) was also found to be useful in generation of infrared radiation for fiber communication applications. The interaction has been analyzed in terms of two independent systems with a perturbation dipole-dipole interaction that may result in an energy transfer process, which effectively sensitizes the Er ions, resulting in the Er emission of infrared light at 1.53–156 μm.[17–21] In bound complex systems, on the other hand, the nanoparticle and the ion must be treated as a single system in which the two species strongly interact to all orders. Under such conditions, the transition lines in the Er ion may not retain their discrete atomistic character, broadening into broad molecular-like bands with spread out oscillator strength. In fact, very little is known experimentally or theoretically about the mechanism of bound complex formation of Si nanoparticles with ions underlying these processes. The stability of complexes against disintegration or fast non-radiative energy dissipation due to Coulomb scattering by the charge centers are in question. It is to be noted that complexes of ions with organic material have been studied for years, but little was performed with semiconductor nanoparticles.[22,23] A better understanding and increased knowledge of the interaction of the nanoparticles with ions in general and magnetic ions in particular can lead to more diverse applications including dual magnetic/optical imaging, optically active diluted magnetic silicon for use in spin-based memories and transistors,[24] and potential infrared generation for use in fiber communications,[17–21] as well as water filtration.[25]

In this paper, we study the interaction and the prospect of forming bound complexes between the heavy magnetic ions of iron or erbium and ultrasmall Si nanoparticles. We examine the robustness and stability of the particle luminescence in ionization environment under strong external electric fields. We perform first principle atomistic calculations employing unrestricted Hartree-Fock density functional theory (UHF-DFT) to examine the interaction and formation of ion-nanoparticle complexes. We calculate the configurations and binding to discern the basic mechanism of the binding.

II. EXPERIMENTAL

The nanoparticles are prepared from Si wafers by chemical etching in HF and H_2O_2 using electrical or hexachloroplatinic acid catalyst.[26,27] In the chemical method, we produce H-terminated red luminescent particles of 2.9 nm in diameter.[27] In the electric method,[26] we produce discrete size Si_nH_x particles that are 1.0 ($Si_{29}H_{24}$), 1.67 (Si_{123}), 2.15, 2.9, and 3.7 nm in diameter. The smallest four particles are ultrabright blue, green, yellow, and red luminescent,

respectively. The hydrogen passivation of the silicon nanoparticles in HF etching procedures is normally marginal, and it exhibits a large density of chemical defects, impurities, and electronic defects, such as dihydride and trihydrides, which are susceptible to ambient conditions. The incorporation of the highly oxidizing agent H_2O_2 in our procedure is the key to reduction of the carbon-based impurities and to formation of a monohydride (Si-H) termination. The reduced susceptibility to oxidation and other ambient attacks was evidenced by FTIR measurements.[28] Theoretically, we used quantum Monte Carlo (QMC) calculations,[29] which employed accurate Hartree-Fock pseudopotentials to confirm that the presence of H_2O_2 in the synthesis solution causes an exothermic reaction such that an H_2O_2 molecule strips two H atoms from adjacent Si sites, forming two water molecules, followed by the movement of the Si atoms to reconstruct to form a monohydride terminated surface. A prototype of 1 nm nanoparticle determined using those QMC simulations has a $Si_{29}H_{24}$ configuration,[30] which consists of a central tetrahedral unit and a shell of 24 hydrogenated Si atoms in the form of hexagons and pentagons. The configuration involves monohydride termination and is stable against further loss of hydrogen because it is at the edge of sp^2 and sp^3 symmetry.[29,30]

Particle solutions are prepared by dissolving the nanoparticles in an appropriate solvent such as isopropyl alcohol (IPA). We use salts of erbium and iron to provide the metal ions of Er^{3+} and Fe^{3+}/Fe^{2+}. Chloride salts of the metals, such as $FeCl_3/FeCl_2$ or $ErCl_3$ are dissolved in water-alcohol solutions. Mixtures of nanoparticles and ions are prepared in common solvents. The Fe^{3+} is a strong oxidizing agent as it strongly strips an electron from other reagents. $FeCl_3$ is used as flocculating and precipitating agent in the treatment of water, precipitating finely divided solids and colloids.

The ionization environment utilized in the measurements is created in an electrically biased stainless steel nozzle. Particle solution is placed in a reservoir that feeds into the nozzle.[31,32] A grounded conducting plate is placed at a distance of ~3 cm from the nozzle. The setup is positioned horizontally to avoid unwanted solution dripping onto the target plate. The nozzle is electrically biased with respect to the plate, which establishes a non-uniform electric field between them. For purely dielectric medium, the electric field at the opening of the nozzle tip may be estimated from the expression $E_0 = V_0/A_1\, r_c\, ln(4h/r_c)$, where A_1 is a numerical factor equal to 0.707, r_c is the radius of curvature of the nozzle (50 μm), $V_0 = 2.2$ kV is the threshold bias voltage at which spraying takes place and $h = 3$ cm is the distance of the tip to the substrate, which gives 8 MV/m. This field is comparable to the breakdown threshold for pure liquids, and higher than the breakdown threshold in liquid in the presence of impurities (~0.1 MV/m). When the nozzle voltage exceeds a certain threshold voltage (~2.26 kV), the material at the tip of the nozzle is ionized with excess positive or negative charge depending on the sense of the biasing and is propelled to the plate. The material gets propelled with a velocity in the range 1–15 m/s,[33] pinned onto the target, and forms a uniform thin nanosolid film. A fiber-optic spectrometer with excitation in the UV region is used to record the luminescence spectra. The structural and optical stability as well as the chemical composition of the constituents arriving at the target are analyzed with luminescence spectroscopy and imaging as well as using Auger electron spectroscopy (AES).

III. RESULTS

We added ion solution incrementally to nanoparticle solution in IPA, while monitoring the luminescence intensity and the spectral distribution. When larger amounts of ions are introduced, aggregation and precipitation of the nanoparticles is observed even with the naked eye. The precipitation is related to complex formation between the nanoparticle and multiple positive metal ions.[34,35] It is known that sheath layers of ions form on charged particles with the thickness of the layer (Debye length) being proportional to the charge on the particle and inversely proportional to the density of the ions. Figures 1(a) and 1(b) give the time development of the luminescence spectrum of the silicon nanoparticles solution after adding a certain amount of Er^{3+}, below the amount that causes significant precipitation. The spectra exhibit a slow enhancement of the luminescence before it saturates after several hours. With time, the 640 nm band rises faster than the 610 nm band, resulting in a red shift of ~10 nm in the center of the combined band. We isolated the complexes from the solvent by drop drying. We repeatedly (ten times) dispensed each time a certain small volume of the mixed colloid on a device quality silicon wafer and let it dry under ambient conditions. A similar film was also formed using

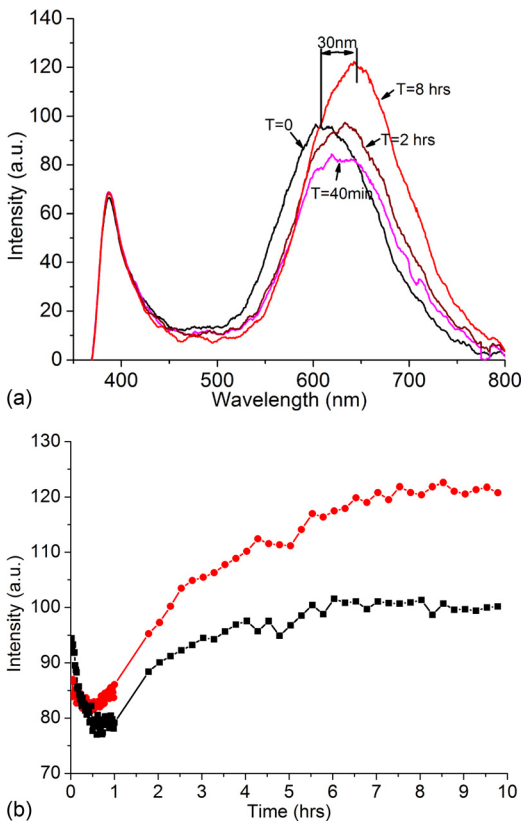

FIG. 1. Time development of the luminescence of silicon nanoparticles dissolved in isopropyl alcohol after adding a certain amount of Er^{3+}. (a) Luminescence spectrum. (b) Intensities of band heads at 610 nm (black squares) and 640 nm (red circles).

a control sample of nanoparticles (without the ions). Luminescent images were taken using 254 nm UV light (not shown). The integrated brightness of the dried film is measured to be 150 counts compared to 100 counts for the control film, consistent with the measured ratio in liquid.

We added Fe^{3+} ion solution incrementally to nanoparticle solution in IPA while monitoring the luminescence intensity and the spectral distribution. When larger amounts of ions are introduced, aggregation and precipitation of the nanoparticles is observed even with the naked eye, indicating the formation of complexes. Figures 2(a) and 2(b) give the corresponding results to those in Figure 1(b) using Fe^{3+} and Fe^{2+} ions with ion concentration below the precipitation point. The figures show enhancements in the luminescence due to complex formation but of smaller magnitude than the erbium enhancement. Unlike erbium, both ions do not have transitions that overlap the visible emission of the nanoparticles. For instance, the electron configuration for Fe^{3+} involves stripping the two 4*s* electrons and one electron from the 3*d* shell of the atom; and Fe^{2+} involves stripping only the two 4*s* electrons. Contrary to the outer orbitals or electrons involved in the iron ions, inner shell *f* orbitals are involved in the erbium ion. Therefore Fe-nanoparticle interaction would be mainly electrostatic. The smaller enhancement of the luminescence observed in the case of Fe^{2+} compared to Fe^{3+} is consistent with the fact that the relative polarizing power for Fe^{2+} is 2.6 compared to 4.7 for Fe^{3+}.[36]

A certain volume of the particle-ion solution is loaded in the nozzle's reservoir. At a positive threshold voltage bias of ~2.26 kV with respect to the counter grounded conducting plate, the colloid is propelled and nanoparticles get pinned down on the substrate, resulting in the formation of a thin film. A nanoparticle-Er^{3+} solution was propelled from the reservoir and formed a film. Figure 3(a) shows a luminescent image of the film, which displays the characteristic red luminescence of the Si nanoparticles, observable by the naked eye under exposure to UV radiation at a wavelength of 254 nm. The luminescence spectrum of the deposited film is recorded and given in Figure 3(b). The pattern on the substrate consists of two regions: a large area corresponding to a deposition cone of ~30°, and a smaller much brighter area corresponding to a ~4°–6° opening angle. The overall brightness is arbitrary but relative brightness is accurate. When the biasing is reversed from positive to negative we find insignificant deposition of silicon nanoparticles, while the nozzle becomes readily clogged. A colloid of nanoparticles and Fe^{3+}/Fe^{2+} ions was also propelled, and nanoparticles get pinned down on the substrate, resulting in the

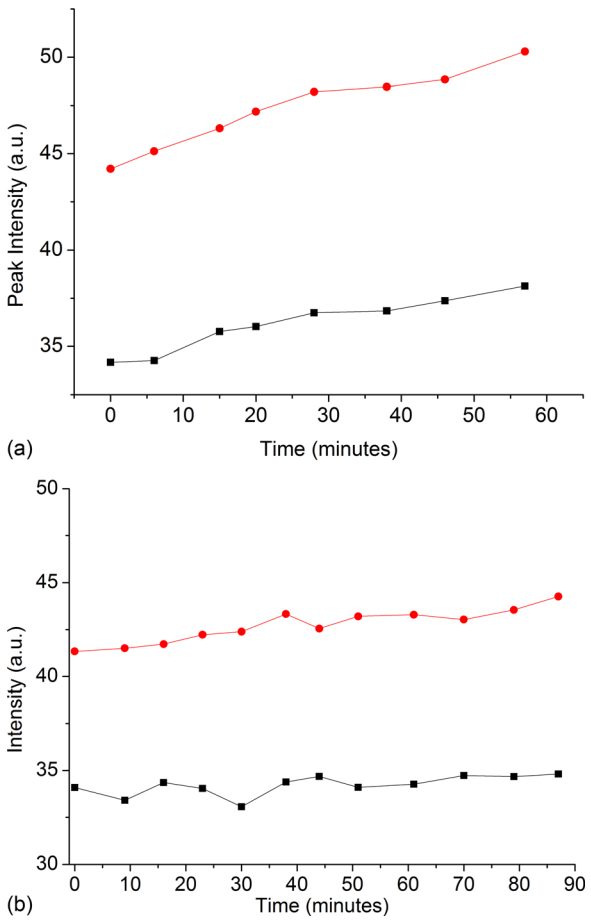

FIG. 2. Time development of the luminescence of silicon nanoparticles dissolved in isopropyl alcohol after adding a certain amount of (a) Fe^{3+} and (b) Fe^{2+} ions. Intensities of band heads at 610 nm (black squares) and 650 nm (red circles).

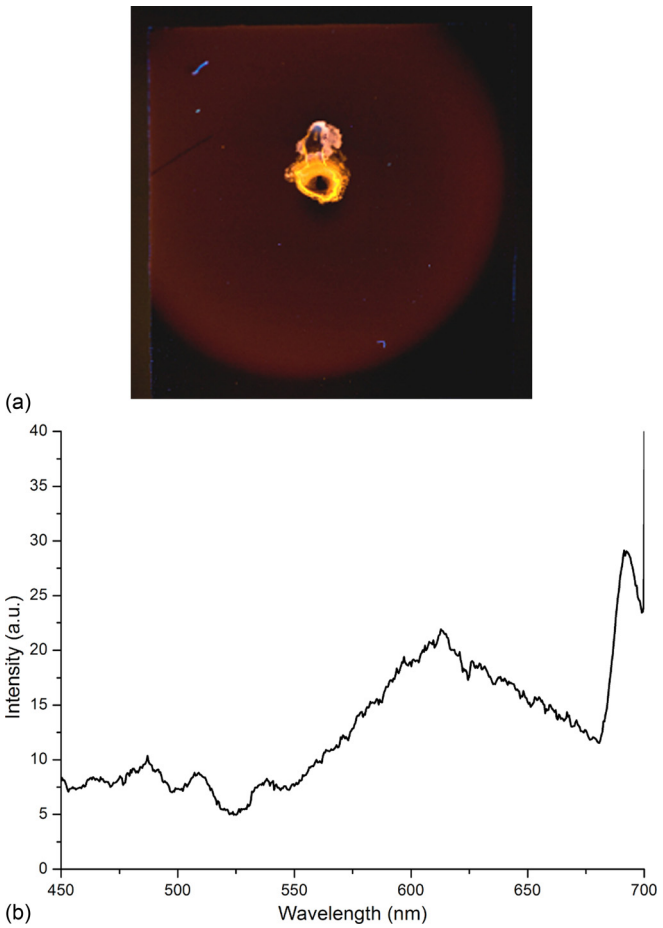

FIG. 3. (a) Luminescent image (2 by 2 cm) of the film produced by electrospray deposition of nanoparticles mixed with Er^{3+} ions (complex) onto silicon wafer coated with titanium under exposure to UV radiation at a wavelength of 254 nm. (b) Corresponding luminescence spectrum of the film taken under excitation of 330 nm.

formation of a thin film. Figures 4(a) and 4(b), respectively, show luminescent images of the film with Fe^{3+} and Fe^{2+}, observable also by the naked eye, under exposure to UV radiation at a wavelength of 254 nm, which displays the characteristic red luminescence of the Si nanoparticles. In these measurements, the Fe ion concentration is significantly less than the Er ion concentration used. Figure 5 is an example photo of scattering from a He-Ne red laser beam traversing the propelled cloud at several distances from the nozzle.

Controlled samples of Si nanoparticles in IPA were also propelled and deposited on a substrate, still exhibiting their characteristic luminescence as shown in Figure 6. In this case, particles are found on the substrate for both positive and negative bias, with the pattern on the substrate consisting of a single deposition cone of 30° angle. We believe that nanoparticles are being charged by deprotonization or complexion with the alcohol negative radical ion $(\text{Si nano-OR})^-$

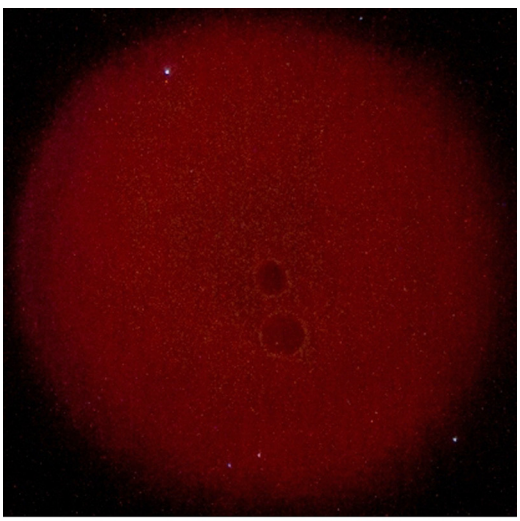

(a)

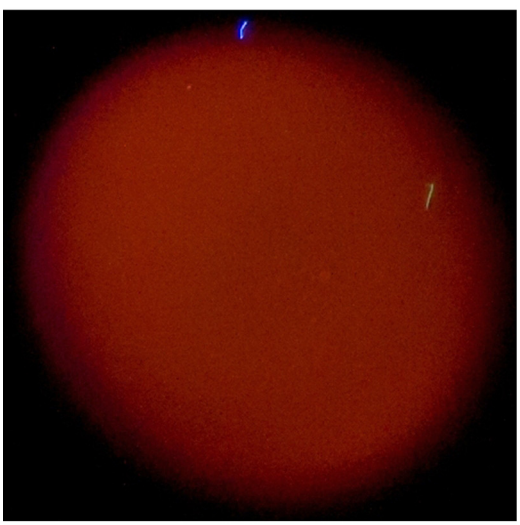

(b)

FIG. 4. Luminescent images (2 by 2 cm) of the film produced by electrospray deposition of nanoparticles mixed with (a) Fe^{3+} and (b) Fe^{2+} ions (complex) onto a silicon wafer coated with titanium under exposure to UV radiation at a wavelength of 254 nm.

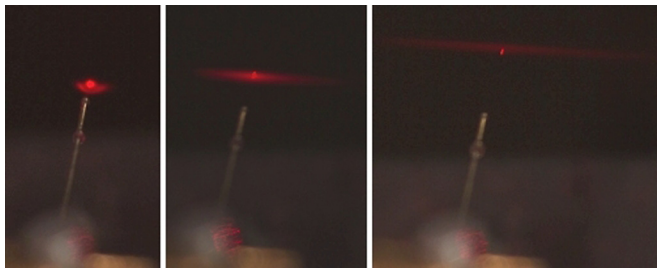

FIG. 5. Photo of scattering from a laser beam traversing the propelled cloud.

or with the positive hydronium ion $(\text{Si nano-}H_3O)^+$, which allows propulsion with both biasing polarities.

We incubated a bundle of fiber glass in a small volume of Si nanoparticle colloid. Upon drying under ambient conditions, the nanoparticles get drawn to the fibers, forming a thin nanofilm. The film is observable by the naked eye under UV irradiation with the luminescence spectrum showing the characteristic emission of Si nanoparticles.[37] This step is followed by a similar incubation process of the coated fibers in an erbium chloride salt solution. The metal ions are drawn to the fibers by electrostatic attraction, forming a metal nanofilm coating over the nanoparticle film. Figure 7 gives the luminescence spectrum taken with excitation using He-Cd laser line at 325 nm of the coated fibers along with the luminescent spectrum of the controlled sample of Si nanoparticles without Er. In addition to the red band characteristics of the nanoparticles, it exhibits absorption dips or holes burned at the absorption lines of erbium ions at 650 nm and 520 nm. Those sharp dips indicate resonant reabsorption. This is unlike the in-solution case in which the luminescence spectrum did not exhibit dip structure at the lines of the free ion (Figures 1 and 3). Enhancement of the luminescence of nanoparticle-ion solution without showing a hole burned at the absorption lines of the ions suggest that

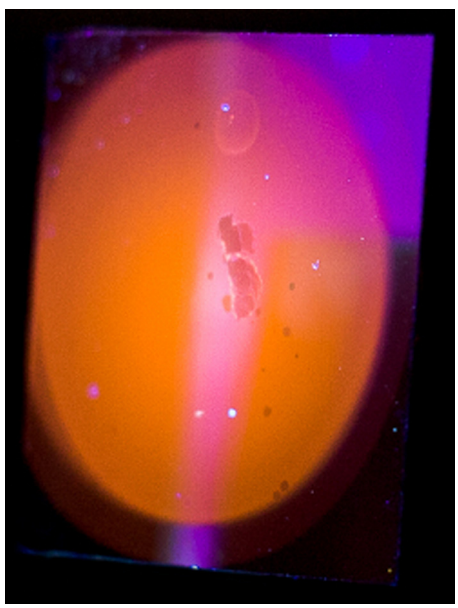

FIG. 6. Luminescent image of the film produced by electrospray from a control Si nanoparticles sample on a silicon wafer (2 by 2 cm) under exposure to UV radiation at a wavelength of 254 nm (arbitrary brightness).

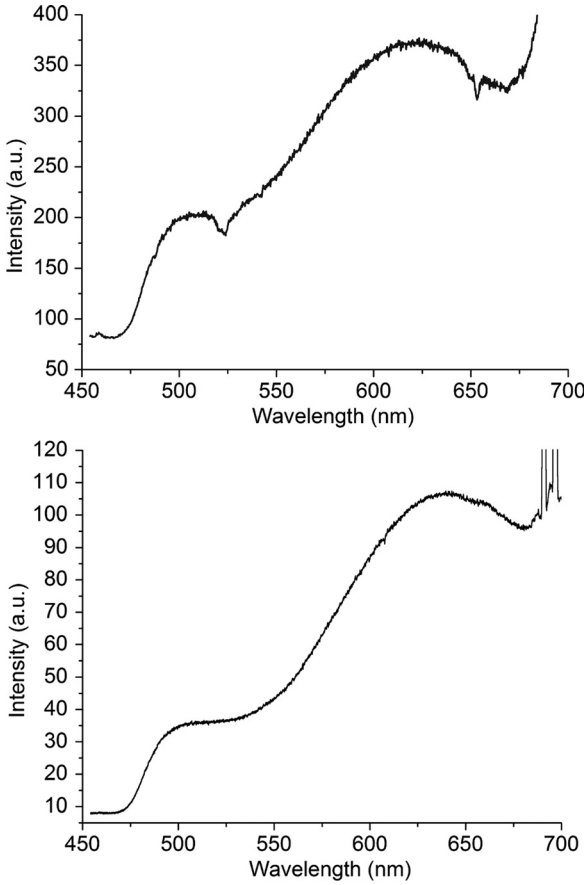

FIG. 7. Luminescence spectrum of fiber glass bundle sequentially incubated in Si nanoparticles and erbium salt (top) and of fiber glass bundle incubated only in Si nanoparticles (bottom). The spectra were taken with excitation at 325 nm of the He-Cd laser line.

a complex ((nano particle-Er)$^{3+}$) has formed, i.e., the two components behave as a single system with strong/close coupling between them, rather than two separate systems interacting optically via emission and re-absorption.

We performed material analysis using AES. Silicon is found across the whole film which is consistent with the luminescence observation. However, erbium is predominantly found in the inner cone with lesser amount in the outer cone, which may indicate more ions per particle in the inner region than the outer region. We used energy dispersive X-ray spectroscopy (EDS) to perform elemental analysis from certain spots on the sample (spatial distribution). The results confirmed the AES results where Er is found predominantly in the inner region, with insignificant amount in the outer region. Moreover, in the measurement the film in the inner cone region showed larger conductivity than in the film in the outer cone, correlating with the distribution of erbium in the film. Theoretical calculations show that the diameter of the deposited area is inversely proportional to the square root of the charge on the droplets.[32] This indicates that nanoparticle-Er complex may consist of multiple erbium ions. Unlike the Er measurements, in the Fe measurements, the low Fe salt density results in less than one Fe ion per particle on the average, producing more uniform film.

The silicon peak in the AES measurement is found as expected at 93 eV. Along with the Si peak, there are weaker peaks at 85 and 104 eV corresponding to different Si-O charge states, indicating some Si-OR terminations resulting from the interaction with the alcohol. We used atomic force microscope to perform topographical characteristics of the film in the outer cone region. A typical line profile across the film gives a thickness of 240 ± 10 nm. At the very outer edges of the film we could find isolated structures of a monolayer or individual structures of 4 nm thicknesses, which correspond to the thickness of a single nanoparticle or complex.

We examined light emission from Er. Optically excited Si nanoparticles embedded in a silicon oxide matrix have been known to effectively sensitize nearby embedded Er ions through a dipole-dipole energy transfer process, resulting in the emission of IR at 1.53–1.56 μm. The crystal field of the oxide matrix breaks the symmetry and makes the otherwise forbidden infrared transitions allowed. An inter particle ion distance of 10 Å makes the transfer process sufficiently strong to observe the infrared radiation. In our present measurements, we used electron excitation at 3 kV and 27 nA current to record the cathodoluminescence. Previously, cathodluminescence from the nanoparticles was observed under electron excitation.[38] Figure 8 presents the spectrum in the range 1400–1700 nm taken with a germanium detector cooled to liquid nitrogen temperature. It shows insignificant sharp emission above the noise level in the region of interest. It is not clear if, in bound complex systems, the transition lines in the erbium ion would retain their discrete atomistic character or they would broaden extensively to form a broad infrared molecular band with spread out oscillator strength. Low temperature photoluminescence measurements with more sensitive infrared detector are being planned.

IV. THEORY

We used the TURBOMOLE quantum computational package to calculate the interaction of Si nanoparticles with heavy ions. The package uses UHF-DFT with a Triple Zeta Valence Plus Polarization (TZVP) basis set and the Becke 3-Parameter Lee-Yang-Parr (B3LYP) functional. In these simulations we used the smaller 1 nm particle as a model calculation because it is small enough to be amenable to such simulations. Nanoparticle-Er^{3+} complexes could be of more interest because they have transitions overlapping the red

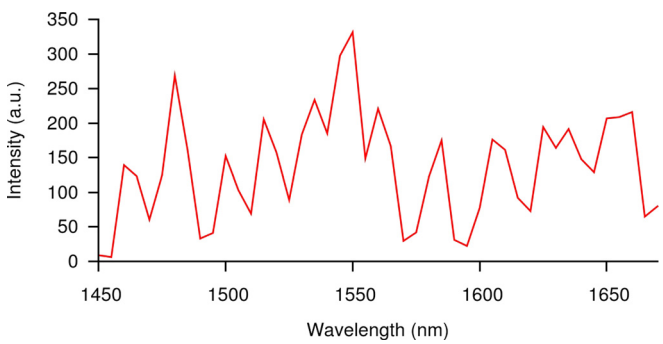

FIG. 8. Cathodoluminescence spectrum in the infrared 1400–1700 nm region taken with 3 kV incident electrons and monitored with a germanium detector at liquid nitrogen temperature.

luminescence band of the particles resulting from partially filled inner shell states. However, we used in the simulation Fe^{2+} instead of erbium ions because simulations using erbium ions are less accurate and harder to implement due to the presence of those partially filled states. The COSMO solvation model was used to handle the liquid solvent.[39]

In Figure 9(a) we present the energy of the complex in solution (water) as a function of the distance of the ion from the center of the Si nanoparticle (the center nuclei) with the distantly separated Fe (+1) ion and a singly charged nanoparticle placed at zero energy. At each distance the structure was relaxed in the 4 unpaired electron configurations. The results show that the polarization of the Si particle induces a sufficient reduction in energy to result in a complex, with the charge of the ion being spread over the particle volume. One local minimum was found at ~−2 eV with the ion penetrating the particle and residing in the interior at a distance of 2.65 Å from its center. A second minimum was found at energy of ~−2.5 eV with the ion resting just outside of the hexagonal Si ring at a distance of 4.25 Å from the center of the particle. The two minima are separated by a potential barrier, which is 0.07 eV and 0.57 eV high from the two minima, respectively. The barrier originates from the breaking through the hexagonal ring. To understand the effect of dielectric screening of water on this potential energy surface, we repeated the calculations in vacuum as given in Figure 9(b). The first minimum becomes deeper with the barrier 0.09 eV above its local minimum energy. The other minimum drops to 0.43 eV below the barrier through the ring, and 1.9 eV below the long distance limit of a Fe(+1) ion and single charged nanoparticle in water. Figure 10 shows the ion-nanoparticle configurations associated with the two minimum energies shown in Figure 9(a).

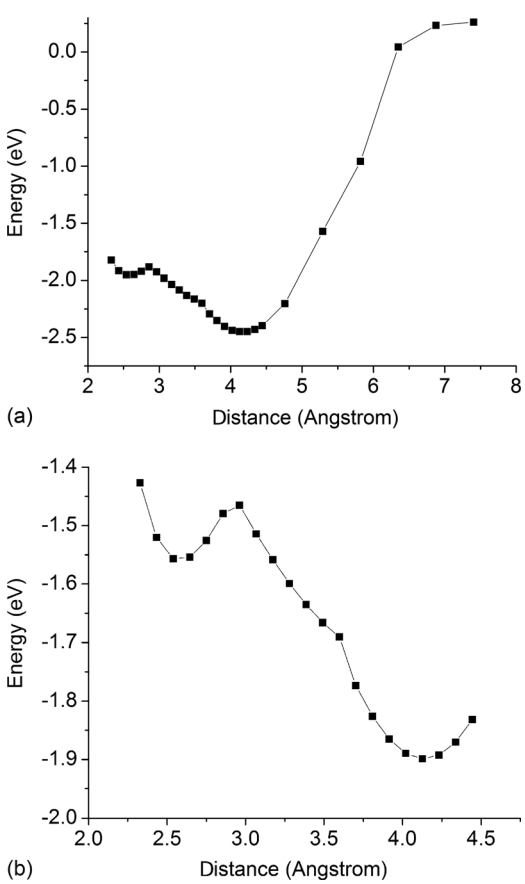

FIG. 9. Calculated total energy of nano-ion complex of 1 nm Si nanoparticle and Fe^{2+} as a function of the distance of the ion from the center of the Si nanoparticle (the center nuclei) (a) in solution and (b) in vacuum.

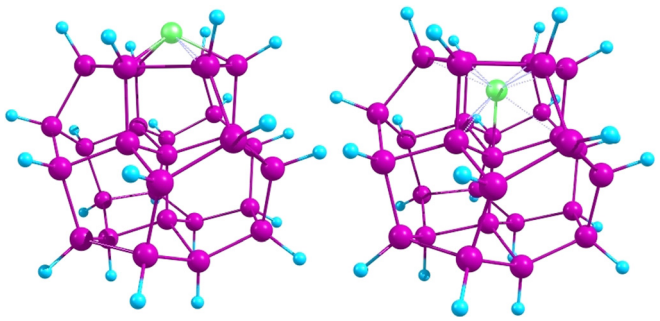

FIG. 10. Schematic of the configurations of the stable complex, showing two minimum energy configurations, one where the ion (green, the lightest color) resides just outside the particle (left) and one where the ion resides just inside the particle (right).

We also examined the possibility of formation of a partially polarized complex of a neutral solvent alcohol molecule and the nanoparticle. The GAMESS quantum chemistry package was used to determine the equilibrium geometry of the polarization-based complex using the Restricted Hartree-Fock (RHF) theory with 6–311G (d, p) basis set.[40] The results give an electrostatic based binding energy of 0.030 eV, comparable to the room temperature thermal agitation energy. The potential drop across the 4 nm particle-IPA complex is estimated to be 32 meV, comparable to the electrostatic binding of the particle to the alcohol molecule as well as to the thermal energy, pointing to instability of the neutral complex.

V. DISCUSSION

As seen in Figures 6 and 3(a), the electrospray deposition of Si nanoparticles in IPA produces one homogeneous luminescent region, while the deposition process of Si-Er mixture shows two regions of different brightness. We believe the inner brighter region is associated with the formation of highly charged Er-nanoparticle complex (multiple erbium ions), while the outer deposition region is associated with lesser charged complexes either with erbium or other radical-complexes. The results also show the stability or enhancement of the brightness (product of absorption and emission efficiencies) upon the introduction of ions, whether under wet conditions or after recovery in the solid phase on the substrate. The fact that the complexes are bright implies that the interstitial Er dopant charge center does not produce strong Coulomb scattering which may dissipate electronic energy non-radiatively. The metal ion however changes the electronic charge distribution in the nanoparticle, breaking symmetries and creating a permanent electric dipole moment. Such redistribution changes the electronic energy of the ground state and the excited states as well as the transition dipole moments between the excited states and the ground state, and consequently the absorption and emission

quantum efficiencies. For example, upon the introduction of the ions, the intensity of the 640 nm luminescence band rises more strongly than that of the 610 nm band, indicating detailed changes in the emission quantum efficiency.

The 1 nm silicon nanoparticle $Si_{29}H_{24}$ has no terminations on its surface with lone electron pairs. Typically ion-molecule complex formation requires lone electron pairs in the ligands of a charge complex, such as an oxide or nitrogen group, to make a coordinate covalent bond. Our calculations show a different mechanism for the case of ion-semiconductor nanoparticle. A ferrous ion may penetrate one of the four hexagonal rings on the surface of a nanoparticle reducing the energy by effectively spreading the charge over the volume of the silicon nanoparticle. The calculations show that the nanoparticles exhibit significant loss of elasticity and the silicon atoms are amenable to large motion making the nanoparticle acquire a large electric polarizability, allowing the ion to penetrate the particle. In fact, the particle is even more polarizable than water, which provides stability of the charge complex. It is also noted that the complex is stable against stripping by the external electric field in the experiment since the binding energy of the ion to the nanoparticles (several eV) is much larger than the 32 meV potential drop across the particles caused by the biasing potential.

At present, there is no available theory that predicts the spraying angles or threshold voltages needed for spray in the presence of metal ions or highly polarizable ultrasmall Si nanoparticles. The threshold bias voltage of the configuration of the nozzle for purely dielectric medium has been previously derived, however.[33] It is given by the expression: $V_0 = A_1\ [2T\ r_c\ \cos\theta/\varepsilon]\ ln(4h/r_c)$, where A_1 is a numerical factor equal to 0.707, T is the surface tension of the liquid, r_c is the radius of the nozzle, ε is the permittivity of vacuum, θ is the Taylor cone angle of the spray ($\sim 49^\circ$ for purely dielectric medium), and h is the distance of the tip to the substrate. Using $r_c = 50\ \mu m$, $\theta = 30^\circ$, and $h = 3$ cm gives $V_0 = 2.2$ kV. For purely dielectric medium, the spray angle is $\sim 49^\circ$ (Taylor cone angle).

Finally, the calculations show that metal ion dopant in the minimum energy configuration is not substitutional. The complex may constitute diluted magnetic nanosilicon, which adds a new dimension to diluted magnetic silicon by providing optical activity. The optical and structural stability of Si nanoparticles against charge particle interactions and collisions including heavy ions, and electrons, and as well as against UV photons[41] is key to technological applications. It is also relevant to the development of current models for the composition of interstellar and interplanetary dust media. Si nanoparticles were proposed as one important component in the corona as well as in interstellar media and that its ionic and charged particle interactions and luminescence under excitation with UV radiation from stars could explain the sizeable wideband background emission that has been observed in the Milky Way and other galaxies, for the last 30 years but never being successfully explained.

VI. CONCLUSION

In conclusion, we subjected silicon nanoparticles of 3 nm across to magnetic ions of Er and Fe in an ionizing field of $\sim$10 MV/m. We have shown that we can produce stable Si nanoparticles-metal ion complex without compromising the luminescence of the nanoparticles. The erbium-nanoparticle complex exhibits a more pronounced enhancement in brightness than the iron complex due to overlap of some transitions of Er ion and the nanoparticle. Atomistic calculations show that the ion forms two stable complex configurations with 1 nm nanoparticles, with the ion either penetrating the particle or residing just outside. The stability of the red visible luminescence indicates that the charge ion center in the complex does not act as center for non-radiative recombination.

ACKNOWLEDGMENTS

We acknowledge the support from NSF Grant ATM 0802499 and NSF Grant OISE 11-03-398. The experiments were carried out in part in the Frederick Seitz Materials Research Laboratory Central Facilities, University of Illinois.

[1]Y. He, C. Fan, and S.-T. Lee, Nano Today **5**, 282–295 (2010).
[2]*Nanosilicon*, edited by V. Kumar (Elsevir, 2007).
[3]*Synthesis, Functionalization, and Surface Treatment of Nanoparticles*, edited by M.-I. Baratron (American Scientific Publishers, 2002).
[4]O. Nayfeh, D. Antoniadis, K. Mantey, and M. H. Nayfeh, Appl. Phys. Lett. **90**, 153105 (2007).
[5]G. Wang, K. Mantey, M. H. Nayfeh, and S. Yau, Appl. Phys. Lett. **89**, 243901 (2006).
[6]Q. Liu, M. H. Nayfeh, and S.-T. Yau, J. Electroanal. Chem. **657**, 172 (2011).
[7]G. Wang, S.-T. Yau, K. Mantey, and M. H. Nayfeh, Opt. Commun. **281**, 1765 (2008).
[8]Y. Choi, G. Wang, M. H. Nayfeh, and S.-T. Yau, Appl. Phys. Lett. **93**, 164103 (2008).
[9]Y. Choi, G. Wang, M. H. Nayfeh, and S.-T. Yau, Biosens. Bioelectron. **24**, 3103 (2009).
[10]A. Smith, G. Belomoin, M. H. Nayfeh, and T. Nayfeh, Chem. Phys. Lett. **372**, 415 (2003).
[11]U. P. Vijh, A. N. Witt, and K. D. Gordon, ApJ **606**, L65 (2004).
[12]U. P. Vijh, A. N. Witt, and K. D. Gordon, ApJ **619**, 368 (2005).
[13]G. Ledoux, O. Guillois, F. Huisken, B. Kohn, D. Porterat, and C. Reynaud, A&A **377**, 707 (2001).
[14]S. R. Habbal, M. Arndt, M. H. Nayfeh, J. Arnaud, J. Johnson, and S. Hegwer, ApJ **592**, L87 (2003).
[15]M. H. Nayfeh, S. Habbal, and S. Rao, ApJ **621**, L121 (2005).
[16]International Innovation May, Paper No. 88, 2012.
[17]M. Fujii, M. Yoshida, Y. Kanzawa, S. Hayashi, and K. Yamamoto, Appl. Phys. Lett. **71**, 1198 (1997).
[18]M. Fujii, M. Yoshida, S. Hayashi, and K. Yamamoto, J. Appl. Phys. **84**, 4525 (1998).
[19]P. G. Kik, M. L. Brongersma, and A. Polman, Appl. Phys. Lett. **76**, 2325 (2000).
[20]P. G. Kik and A. Polman, J. Appl. Phys. **88**, 1992 (2000).
[21]P. G. Kik and A. Polman, Mater. Sci. Eng. B **81**, 3 (2001).
[22]F. Artizzu, M. L. Mercuri, A. Serpe, and P. Deplano, Coord. Chem. Rev. **255**, 2514 (2011).
[23]W. Kaim, Coord. Chem. Rev. **255**, 2503 (2011).
[24]S. Pearton, Nature Mater. **3**, 203 (2004).
[25]E. E. Nuxoll, M. A. Hillmyer, R. Wang, C. Leighton, and R. A. Siegel, ACS Appl. Mater. Interfaces **1**, 888 (2009).
[26]G. Belomoin, J. Therrien, A. Smith, S. Rao, S. Chaieb, and M. H. Nayfeh, Appl. Phys. Lett. **80**, 841 (2002).
[27]D. Nielsen, L. Abuhassan, M. Alchihabi, A. Al-Muhanna, J. Host, and M. H. Nayfeh, J. Appl. Phys **101**, 114302 (2007).
[28]Z. Yamani, H. Thompson, L. AbuHassan, and M. H. Nayfeh, Appl. Phys. Lett. **70**, 3404 (1997).
[29]G. Belomoin, E. Rogozhina, J. Therrien, P. V. Braun, L. Abuhassan, M. H. Nayfeh, L. Wagner, and L. Mitas, Phys. Rev. B **65**, 193406 (2002).

[30]L. Mitas, J. Therrien, R. Twesten, G. Belomoin, and M. H. Nayfeh, Appl. Phys. Lett. **78**, 1918 (2001).
[31]P. Kebarle, J. Mass Spectrom. **35**, 804 (2000).
[32]W. Yang, B. Lojewski, Y. Wei, and W. Deng, J. Aerosol Sci. **46**, 20 (2012).
[33]A. A. Naqwi, R. P. A. Hartman, and J. C. M. Marijnissen, Part. Part. Syst. Charact. **13**, 143 (1996).
[34]M. Keidar and I. Beilis, IEEE Trans. Plasma Sci. **38**, 3249 (2010).
[35]P. Berger, N. B. Adelman, K. J. Beckman, D. J. Campbell, A. B. Ellis, and G. C. Lisensky, J. Chem. Ed. **76**, 943 (1999).
[36]M. M. El-Desoky, K. Tahoon, and M. Y. Hassan, Mater. Chem. Phys. **69**, 180 (2001).
[37]K. Mantey, M. H. Nayfeh, B. Al-Hreish, J. Boparai, A. Kumar, L. D. Stephenson, A. J. Nelson, S. A. Alrokayan, and K. M. Abu-Salah, J. Appl. Phys. **109**, 064321 (2011).
[38]L. Abuhassan, M. Khanlary, P. Townsend, and M. H. Nayfeh, J. Appl. Phys. **97**, 104314 (2005).
[39]V. S. Bryantsev, M. S. Diallo, A. C. T. van Duin, and W. A. Goddard III, J. Phys. Chem. A **112**, 9104 (2008).
[40]O. M. Nayfeh, D. A. Antoniadis, K. Mantey, and M. H. Nayfeh, Appl. Phys. Lett. **94**, 043112 (2009).
[41]K. Mantey, M. Kwit, M. H. Nayfeh, A. Kumar, L. D. Stephenson, and A. J. Nelson, J. Appl. Phys. **107**, 064316 (2010).